
Article:
Hinton, J orcid.org/0000-0003-1047-7315, Dejan, B, Mirgkizoudi, M et al. (3 more authors) (2019) Hybrid additive manufacturing of precision engineered ceramic components. Rapid Prototyping Journal, 25 (6). pp. 1061-1068. ISSN 1355-2546

https://doi.org/10.1108/RPJ-01-2019-0025

Abstract

Purpose – This paper summarizes the development of a hybrid additive/subtractive manufacturing platform for the production of full density ceramic components.

Design/methodology/approach – Fabrication of a fully dense ceramic components is achieved using 96% Al_3O_2 ceramic paste extrusion and a planarizing machining operations. Sacrificial polymer support can be used to aid the creation of overhanging or internal features. Post-processing using a variety of machining operations improves tolerances and fidelity between the component and CAD model whilst reducing defects.

Findings – This resultant three-dimensional (3D) monolithic ceramic components demonstrated post sintering tolerances of ±100µm, surface roughness's of ~1µm Ra, densities in excess of 99.7% and three-point bending strength of 221MPa.

Originality/Value – This method represents a novel approach for the digital fabrication of ceramic components, which provides improved manufacturing tolerances, part quality and capability over existing additive manufacturing approaches.

Introduction

Precision engineered ceramics are used across a diverse range of industrial sectors including healthcare (Hollister, 2005), electronics (Buchanan, 1986), power generation and storage (Correia et al., 2013), chemical and processing (Hammel, Ighodaro and Okoli, 2014), aerospace (Naslain et al., 2004) and automotive (Brosha et al., 2002). Compared to polymers and metals, ceramics exhibit superior mechanical properties including excellent electrical and thermal insulation, biocompatibility, high resistance to heat, corrosion, erosion and wear (Wachtman, Cannon and Matthewson, 2009). However, these characteristics reduce the processability of the bulk ceramic material, resulting in only minimal material removal operations and no formative processing being suitable. Instead, ceramic powders are dispersed within a carrier typically consisting of solvent solutions or matrix materials. The resultant feedstock can be readily processed using a range of manufacturing processes such as extrusion (Ribeiro, Ferreira and Labrincha, 2005) or injection moulding (Edirisinghe and Evans, 1986). However, the use of moulds and component specific tooling impose significant design constraints, prohibit the formation of internal structures and require volume production to be economic viability (Tay, Evans and Edirisinghe, 2003). AM processes capable of processing engineering ceramics have demonstrated a way to overcome these restrictions but further innovation in terms of the range of processable materials, greater part density and minimising shrinkages is still required to meet the demands of producing precision ceramic components.

Powder-based processes present an obvious solution for the production of ceramic components owing to the prevalence of ceramics powder within conventional feedstock preparations. AM Processes that use thermally-induced binding mechanisms for the direct processing of ceramic powder, such as selective laser sintering (SLS) and selective laser melting (SLM), require high sintering temperatures (Klocke and Ader, 2003; Wilkes et al., 2013). As a result, these approaches suffer from thermally induced stresses, part cracking and poor process control, thus driving the majority of research to focus on methods that produce green-state parts. Powder bed methods using either indirect SLS to fuse a sacrificial polymer binder coating on the ceramic powder particles or binder jetting a liquid bonding agent to selectively join the powder have been used to manufacture a variety of parts including tissue scaffolds (Cox et al., 2015) and industrial catalysts (Parra-Cabrera et al., 2017). A key benefit of these processes is the self-supporting nature of the process, mitigating the need for secondary support structures (Deckers, Vleugels and Kruth, 2014). However, the need to maintain feedstock flowability when using a powder based material often results in components having a rough or pitted appearance and containing a high degree of porosity (Qian and Shen, 2013; Gonzalez et al., 2016).

One promising approach for the 3D digital fabrication of ceramics is stereolithography (SLA) which involves the selective curing layer-by-layer of a photo-curable monomer containing a homogeneous dispersion of ceramic powder. The process can achieve a low surface roughness (0.84µm R_a), fine features (100µm), tight

geometric tolerances (100-125μm) and high densities (99.7%) but the additional ceramic material causes modification to the rheological properties and processing characteristics of the monomer (Martin and Johannes, 2014). Consequently, the volume of ceramic that can be dispersed is limited and shrinkages up to 30% can be experienced during thermal processing which is significantly higher than conventional ceramic manufacturing methods which are typically 16-18% (Shui, Zeng and Uematsu, 2006). Moreover, the type of ceramic material alters the degree of absorption, thus restricting the use of darker materials (Halloran, 2016).

Material extrusion (ME) which selectively dispenses a suitable feedstock through a nozzle or orifice to form a continuous bead of material has been shown to fabricate high density ceramic parts using a wide range of ceramic materials (Bellini, 2002), slurries (Cesarano III, 1999), hydrogels (Feilden et al., 2016) and sol-gels (Owen et al., 2018). When compared with SLA, ME can process higher loadings of ceramic material, up to 75vol%, thus reducing shrinkages during the sintering stage (Gao et al., 2015). Lower shrinkages reduce the possibility of deformation and cracking during debinding and sintering, enabling larger and more complex geometries to be successfully fabricated (Sikalidis, 2011). Additionally, ME processes can achieve production rates of up to 20cm^3/hour and provides convenient multi-material deposition enabling the creation of functionally-graded structures (Peng, Zhang and Ding, 2018; Abel et al., 2019). However, the resolution of this approach is limited by the minimum diameter of the nozzle, which is controlled by the particle size of the dispersed material. Subsequently, parts typically exhibit significant stair stepping with minimum features of ±300μm. Sheet lamination has been used to fabricate ceramic components using tape cast sheets which are selectively cut and stacked to form individual layers (Gibson, Rosen and Stucker, 2010). However, stacking alignment, restrictive minimum feature size and tolerances plus problematic removal of excess material restrict the geometries that can be fabricated (Klosterman et al., 1998).

In summary, each AM approach in isolation currently has restrictions in terms of material compatibility, resolution, density, scalability or component performance. One route to overcome these limitations is a combinatorial manufacturing approach where multiple digitally driven processes are interleaved to create a single, integrated system (Lorenz et al., 2015). To-date, these manufacturing approaches have been prevalent in the metal AM systems, but as yet have not been widely implanted for the production of engineering ceramics (Soares et al., 2018). This paper presents a hybrid AM approach where both additive and subtractive computer controlled processes are integrated together resulting in a process that has the flexibility of additive manufacturing with the surface finish and tolerances achieved using subtractive processes.

Materials and Methods

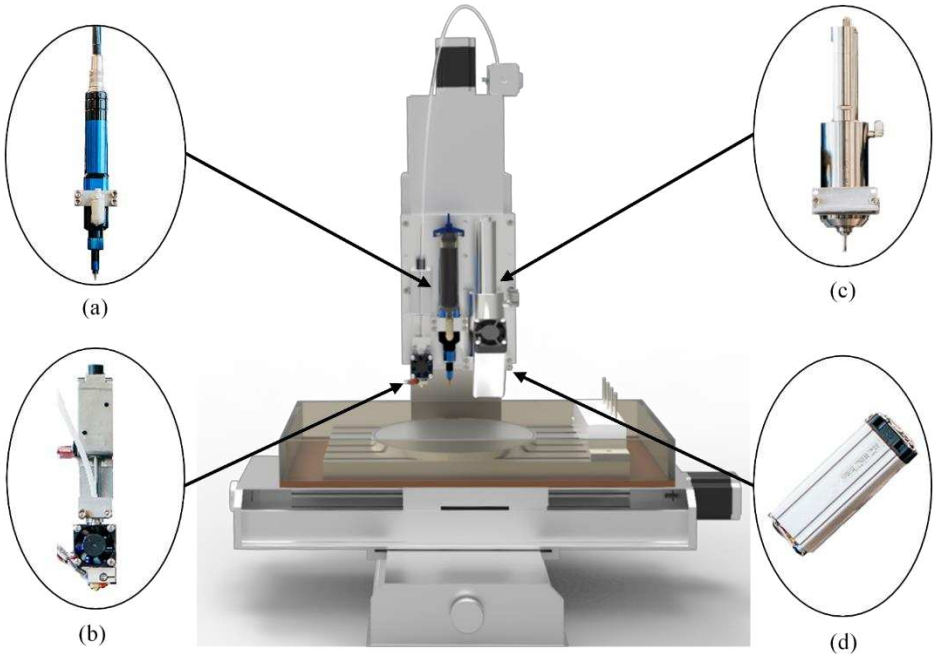

Figure 1 – CAD rendering of the hybrid manufacturing equipment (a) high viscosity paste dispenser (b) hot end and extruder for sacrificial support generation (c) machining spindle and automatic tool changer for subtractive processing (d) forced convection drying unit for accelerated drying of the deposited ceramic paste.

Figure 1 shows a CAD rendering of the hybrid manufacturing equipment. The process was developed using 96wt% alumina with an average primary particle size of 2-3µm. The raw feedstock has been formulated into a high viscosity, aqueous paste with a measured moisture content of between 18-22%, using a proprietary binding medium developed by Morgan Advanced Materials. Sacrificial support was produced using a commercially available hot end (E3D V6, UK) and extruder (Bulldog Lite, UK) with 1.75mm PLA filament. Subtractive milling operations are achieved using a precision, high speed micro-machining spindle (Nakanishi EM-3060J, Japan) with an automatic tool changer (Nakanishi NR50-5100 ATC, Japan). Other elements of the system include a heated convection drying unit for accelerated drying of individual layers. The dispensing and machining hardware have been mounted to a 3-axis CNC stage. The various elements of the system are controlled using commercially available, Mach3 CNC software (Newfangled Solutions, USA). Toolpaths for the additive elements were generated using open source slicing software whilst the subtractive elements were generated using CNC CAM software, which are subsequently amalgamated into a single file, enabling the manufacture of components to be independent of operator input. Once fabricated, the green-state components are thermally processed at a peak firing temperature of 1400°C.

Component Analysis and Metrology

Analysis of components was undertaken post fabrication and post sintering. Geometric dimensions were measured using a non-contact laser profile scanner (micro-epsilon, Germany), surface roughness was determined using 3-dimensional focus-variation measurements (InfiniteFocus, Alicona, Austria) and the mass was measured using a 0.1mg accuracy micro-balance (Practum®, Sartorius, Germany). Analysis of the post sintered components involved the comparison of the pre and post sintering dimensions to determine the relative shrinkages as a result of the thermal processing. The density of the sintered samples was calculated using the Archimedean technique using a density determination kit in conjunction with a ±0.1mg accuracy micro-balance (Practum®, Sartorius, Germany). 25% of the samples were selected at random and sectioned in order to examine internal structures. Mechanical strength was determined using three-point bending of test specimens measuring 5mm x 5mm x 50mm. The test parameters were derived from production tests used by Morgan Advanced Materials (Z005, Zwick/Roell, Germany). Jigs supporting the specimens were located 40mm apart and a preload force of 10N was applied. The deflection mechanism moved at a rate of 1mm/min.

Material Characterisation

This hybrid manufacturing approach represents an advancement over existing systems as a range of materials can be processed by formulating the ceramic powder into a viscoelastic paste. The precursor ceramic paste exhibits a high resting viscosity owing to the high volume of ceramic material and carrier rheology. To extrude the paste, it is required to exhibit shear-thinning behaviour. The viscosity is required to rapidly return to a sufficiently high value on removal of the shear to obtain good shape retention and prevent deformation. Characterisation of rheological properties was investigated using an MCR 102 parallel plate rheometer (Anton Paar, Austria). Figure 2 shows the shear thinning behaviour of the material which was subjected to shear rates between 50-500/s, thus confirming the materials suitability for extrusion-based processes.

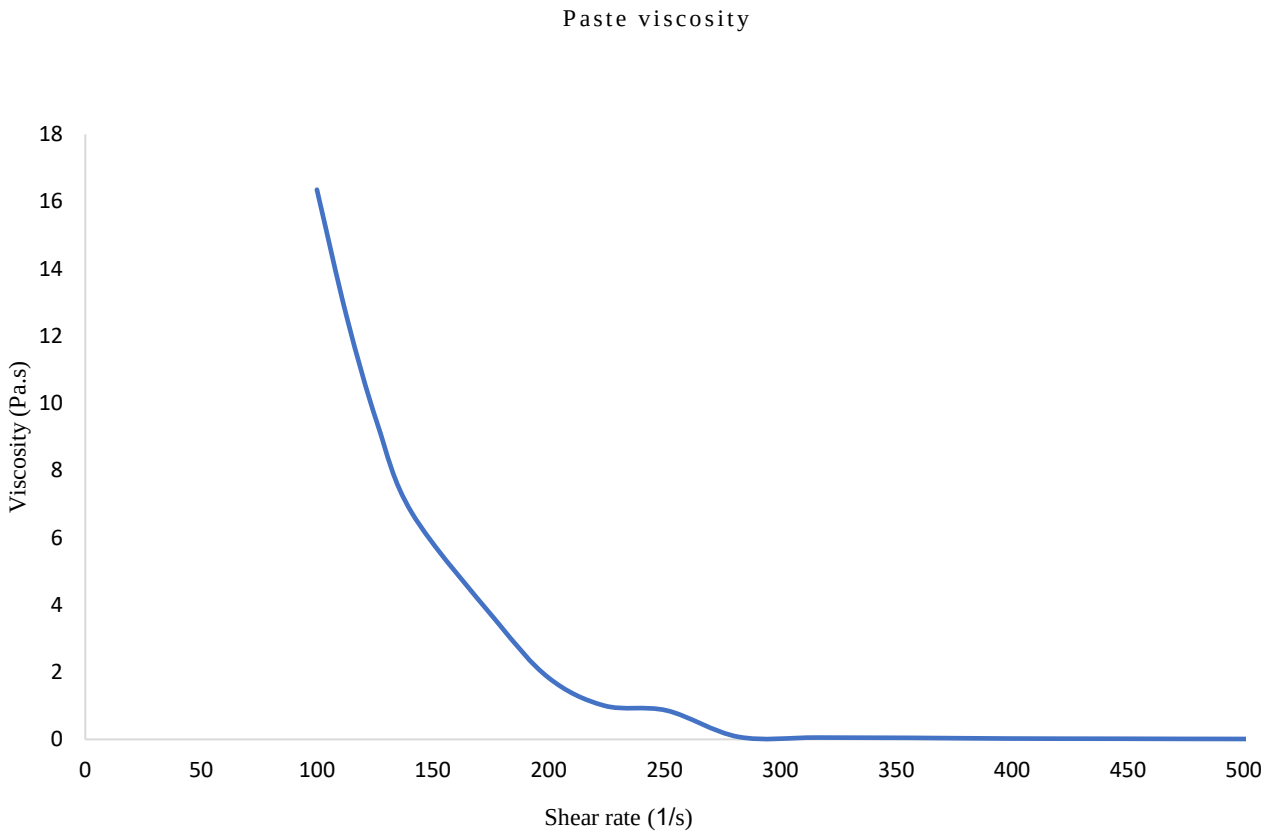

Figure 2 – Formulation of ceramic materials into non-Newtonian shear-thinning pastes enables a wide range of materials to be readily processed using extrusion type processes.

Process Design

Auger-screw dispensing systems were identified as being most suitable due to the additional pre-shearing and mixing, improving the consistency of the extruded material and giving the ability to reverse the flow to stop erroneous deposition. Tapered rather than straight nozzles were identified as being the most suitable as these prevented excessive shear thinning of the paste, resulting in faster build rates and improved shape retention. Atmospheric drying of the paste was noted as the dominant factor affecting build rate. Accelerated drying achieved through the addition of a heated forced convection drying unit resulted in drying times decreasing from several minutes to several seconds. To achieve uniform drying across the surface of the part and to prevent the formation of hotspots, the drying unit was rastered across the part.

Results and Discussion

Manufacturing Process

Initial investigation of the ceramic deposition process was undertaken using a 25 gauge (437µm) tapered nozzle using extrusion rates between 80 to 120µL/min and nozzle speeds between 380 and 470mm/min. 30mm tracks were deposited onto a PLA substrate, with 3 repeats of each track being made to mitigate any randomly occurring defects. Between sets, the nozzle speed was increased in increments of 5mm/min whilst the material flow rate was decreased in increments of 2µL/min. The nozzle height remained constant through all tests at a height of ½ nozzle diameter. The tracks were analysed using focus-variation measurements taking 2mm long

measurement profiles at 7mm intervals. The tracks were assessed based on consistency and profile dimensions. An extrusion rate of 104µL/min with a nozzle speed of 420mm/min was found to create a consistent cross-sectional profile with suitable dimensions to produce fully dense parts. Figure 3 illustrates the process flow for the fabrication of precision engineered ceramic components.

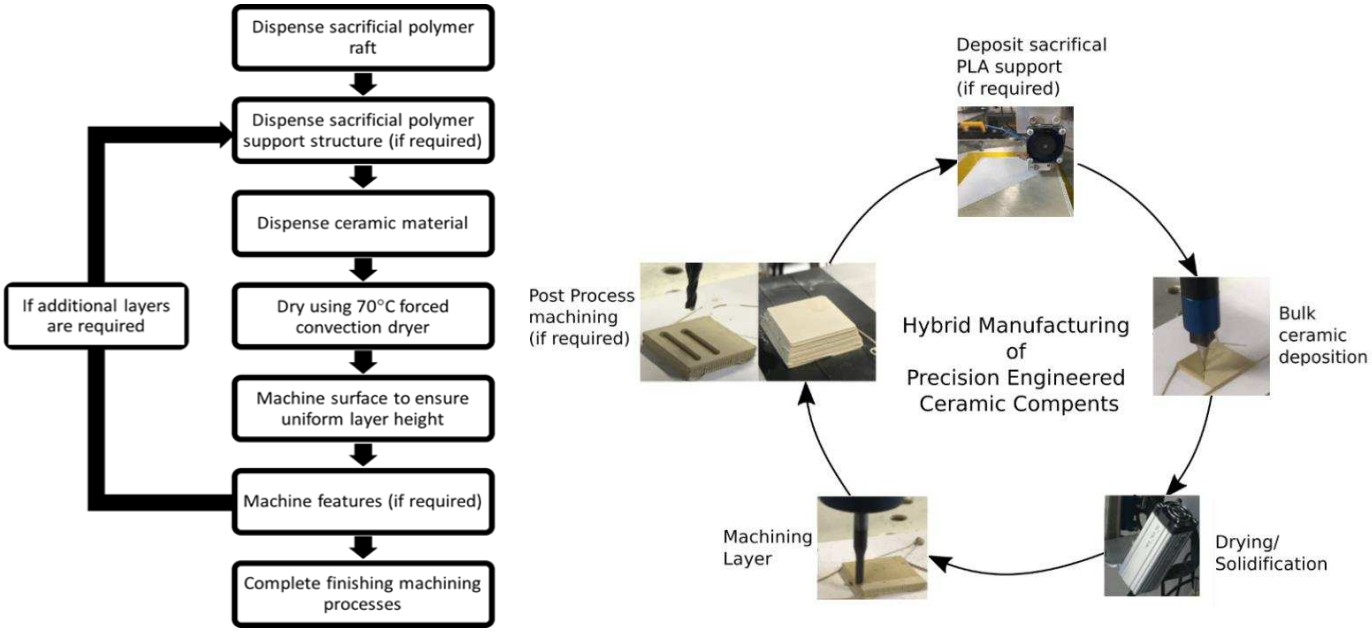

Figure 3 – The process flow for the hybrid manufacture of ceramic components. (left) Process of manufacturing ceramic components and adding additional features using subtractive processes.

The drying characteristics of the paste were investigated through the production of samples measuring 30mm x 30mm x 3mm. Accelerated drying is advantageous to reduce fabrication times as air drying of the part under ambient conditions was assessed to be up to 5 minutes per layer. A heated forced convection unit with 3 fan speeds and variable temperature control was used at varying distances from the part. Parameters were investigated by increasing the distance between the heating unit and part from 50-300mm in 50mm increments. 6 Repeats of the test were undertaken altering the speed and the temperature of the drying unit. The heat was initially applied for 10 secs before being removed and visually inspecting the part. If insufficient drying had occurred the heat was reapplied, in 10 sec increments until a homogeneous surface had formed on the part. During these investigations it was found that rapid heating of the component could result in cracking due to non-uniform heating of the component. Conversely, fast air flows caused rippling and deformation of the drying material, due to the formation of a surface skin before the bulk layer has fully dried. The drying characteristics were validated by assessing the machining characteristics by planarise machining of the surface. The identification of the optimum test parameters resulted in the fitting of a 70°C enclosure heater at a height of 80mm. Drying times were calculated to be less than 30 seconds for each 400µm thick layer with an area of 200mm^2.

Investigation of machining parameters commenced with tests to determine the suitability of cutting tools and cutting tool materials. Conventional fluted High Speed Steel (HSS) tooling proved unsuitable due to rapid dulling and excessive wear on the tool, however, the fluted tooling resulted in good edge retention and feature production. Switching to CVD diamond coated tooling retained the excellent machining characteristics and improved tooling life. Adoption of fluted cutting tools required investigation of climb and conventional milling operations. Climb milling involves the cutter rotating with the feed whereas conventional milling involves the cutter rotating against the feed. Feedrates ranging from 150-700mm/min and spindle speeds ranging from 6,000-12,000 RPM were investigated. The operations were judged visually using edge retention and quantitatively using surface roughness and geometric tolerances. End milling is used for planarizing and finishing operations, to level surfaces relative to the tooling and remove surface defects. End milling demonstrated no significant variation in surface roughness with all components exhibiting a degree of tooling marks with R_a values measuring 1.62µm for climb milling and 1.69µm for conventional milling. Both processes demonstrated good edge retention with no defects attributed to the machining operation. Side milling operations are

used to post-process the components to remove stair-stepping and any defects that may have occurred on the periphery of the part. Side milling operations revealed considerable difference between surface roughness and edge retention due to the interaction of the cutting surface and the part. The measured R_a of climb milling was significantly less than that of conventional milling with values of 1.11μm and 2.43μm respectively. Visually, parts machined using conventional milling exhibited striations and other defects attributable to the machining process. Consequently, deteriorated edges caused parts to have less defined profile with an increased chance of cracking during thermal processing. Comparison with non-machined samples with an average R_a value of 8.09μm confirmations the merits of post process machining.

The manufacture of components with more complex and conformal surfaces requires the use of additional tooling and machining operations. The production of conformal and tapered geometries demonstrates the capability of the system to produce 3D geometries. Post process machining using a ∅1mm ball nose cutter to remove the stair stepping improves the aesthetics and accuracy of manufactured parts. The production of high accuracy features can be realised by slot milling and drilling. These operations are used to machine channels and holes into the part, by lowering the cutting tool in the Z direction and in the case of slot milling, translating the cutting tool to form a channel. Consequently, these operations introduce plunge rate as an additional parameter. Plunge rate is the rate at which the cutting tool moves downward through the component. Plunge rates ranging from 30-70mm/min was investigated using end mills and 45-325mm/min for drills using a spindle speed of 12,000RPM. The features were assessed using the same techniques and criteria as the previous tests. The tests identified optimum plunge rates of 50mm/min for end mills and 220mm/min for drills.

Manufactured Components

Validation and optimisation of the system's capability was achieved through the production of components demonstrating a range of geometries and features. The components were fabricated on a PLA raft, deposited by the in-situ polymer extruder. During the production of components, the suitability of PLA as a sacrificial support material was confirmed by the production of overhanging features and sufficient adhesion between the deposited PLA and green ceramic material. Figure 4 (a) shows square green-state tiles measuring 30mm x 30mm x 6mm. These components were used to optimise machining parameters such as slot milling (centre) and drilling using 2 sizes of drill bits (right). Figure 4 (e) shows the components post firing, which measure 25mm x 25mm x 5.2mm. Figure 4 (b) shows green-state flat top pyramids with the base measuring 30mm x 30mm, height of 10mm and top measuring 20mm x 20mm. These samples were used to demonstrate the merits of post-process machining using a ∅1mm ball nose cutter. The specimens illustrate varying degrees of post process machining. The left-hand part shows a pyramid with no post-process machining. The centre and right-hand parts demonstrate increasing levels of post-process machining, demonstrating the merits of in-situ post processing. Figure 4 (f) shows the components post firing which have a measured base of 25.5mm x 25.5mm and height of 8.6mm. Figure 4 (c) shows the complex and conformal geometries that were fabricated using all elements of hybrid process. The components include a pyramid with a height of 20mm and base of 30mm x 30mm, a hollow hemisphere with an outer diameter of 28mm and a wall thickness of 4mm. Figure 4 (d) shows an overhanging bridge structure with a span of 8mm, using PLA as a sacrificial support material. Figure 4 (h) shows the overhanging post sintering, with no visible PLA residue or deformation.

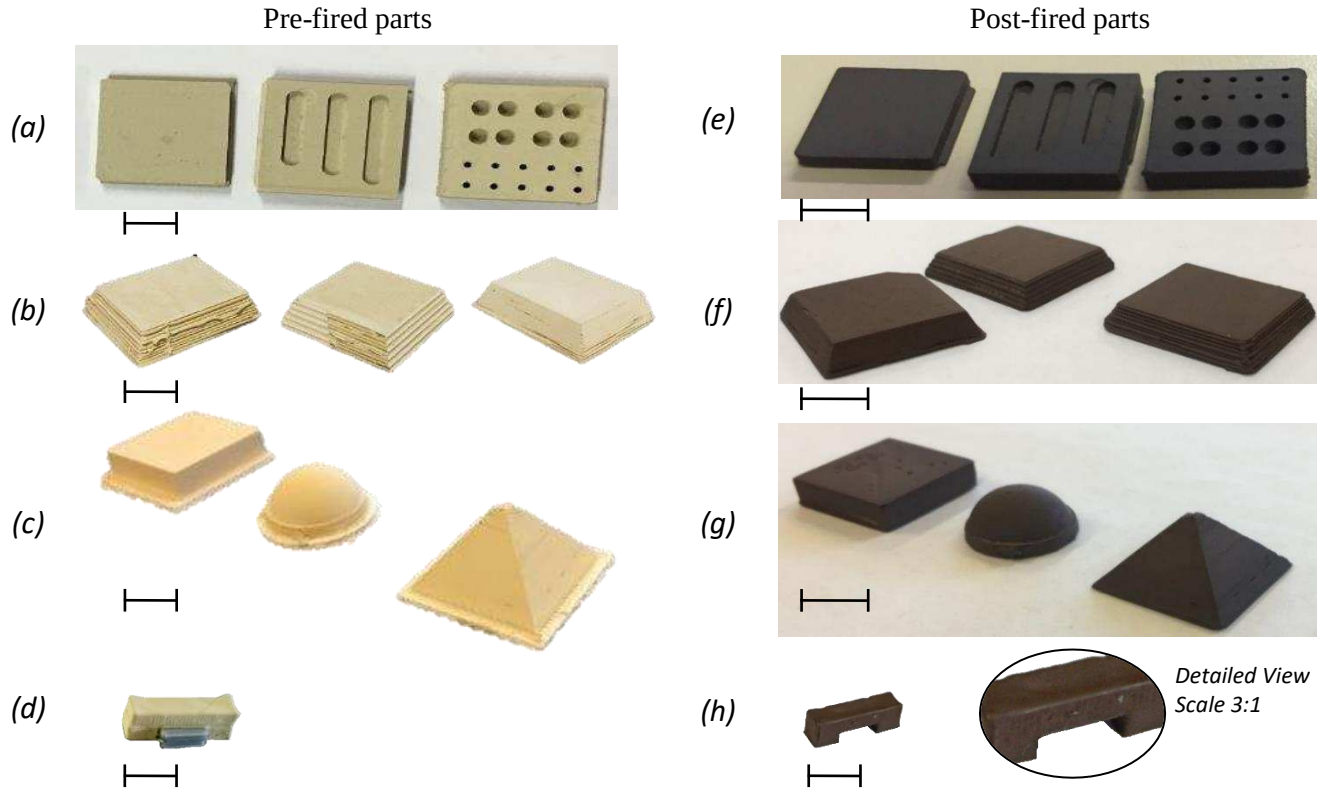

Figure 4 – Shows a range of components and features s fabricated using the hybrid manufacturing process. (a) shows square tiles in the green state with machined slots and drilled holes. (b) shows flat top pyramids in the green state with increasing levels of post process machining. (c) shows green state 3D geometries including a tile, hollow hemisphere and solid pyramid. (d) Shows an overhanging bridge structure using a sacrificial PLA support structure. (e-h) shows the components post firing with measured shrinkages of between 16-18%.
Scale bar = 10mm

Geometric measurements of the green and sintered components were obtained using a non-contact laser scanner. The measurements showed that the components had been fabricated to a resolution of ±100µm. Comparison of the measured values from green-state and sintered parts enabled the calculation of linear shrinkage, which was calculated to be between 16-18%. Surface roughness measurements of the components shown in Figure 4 (a) were used to optimise the machining parameters. Figure 5 show the results of tests in which feedrate was varied and spindle speed was at 10,000 RPM. During these tests spindle speed (RPM) was varied from 6,000-12,000 RPM in 500 RPM increments. The tests identified a feedrate of 330mm/min with a spindle speed of 12,000 RPM as providing optimum results thus, resulting in the lowest surface roughness with best edge profiles.

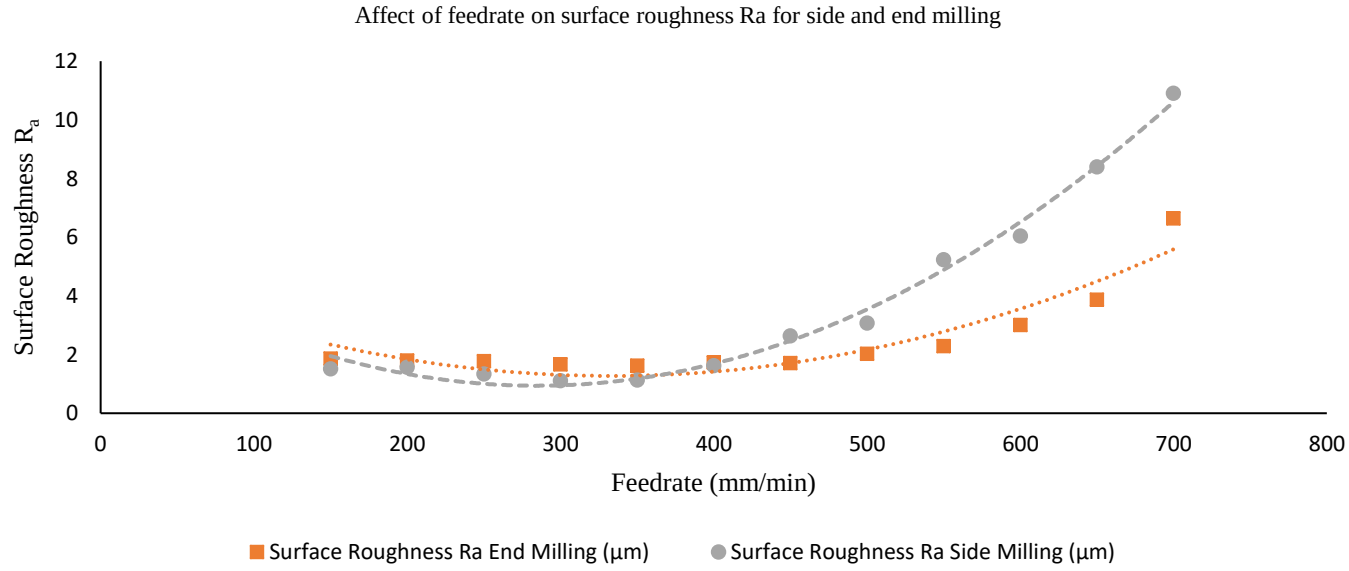

Figure 5 – The effect on surface roughness as a result of changing the federate of the spindle for both side and end milling operations

To determine the mechanical strength, 20 bend test samples measuring 6mm x 6mm x 60mm were manufactured in a single batch. A single batch was used to facilitate direct comparison between the different components. It should be noted that the test bars weren't polished or chamfered, which would minimise the effect of surface cracks and defects. 3-point bend testing of the fabricated specimens were shown to exhibit an average bend strength of 221MPa with a maximum of 253MPa. The results are comparable to other additively manufactured components (Denham et al., 1998), but show a reduction compared to conventionally manufactured parts (Ćurković et al., 2010). Albeit these figures are very encouraging, further improvements to the samples mechanical strength could be achieved by conducting secondary post processing such as polishing and chamfering of the test specimens.

Post-sintering, the density of the components was determined following the same protocol used in production by Morgan Advanced Materials. The density determination apparatus, in conjunction with a 0.1 mg microbalance enabled the volume of the manufactured components to be calculated. The results showed that the components had <0.5% porosity. Further analysis of the sintered components revealed densities of 99.7%, which was validated by analysis under SEM. Figure 6 (a) shows half of a bend test sample that was used to obtain the surface roughness data interlayer region sinter fully to yield a monolithic component. Figure 6 (b) shows the cross-section of the bend test sample along the break interface. The interface shows a number of 10-20µm pores attributable to insufficient degassing during the packing of the material. Figure 6 (bottom row) shows the results of the surface roughness assessment on a bend test sample. Figure 6 (c) shows the surface profile of the top surface that has been machined using an end milling operation. Figure 6 (d) shows the surface profile for the edge of the component that has been machined using climb milling. Figure 6 (e) shows the underside of the test samples that hasn't been machined. The markings are a result of dispensing the ceramic directly onto a PLA substrate.

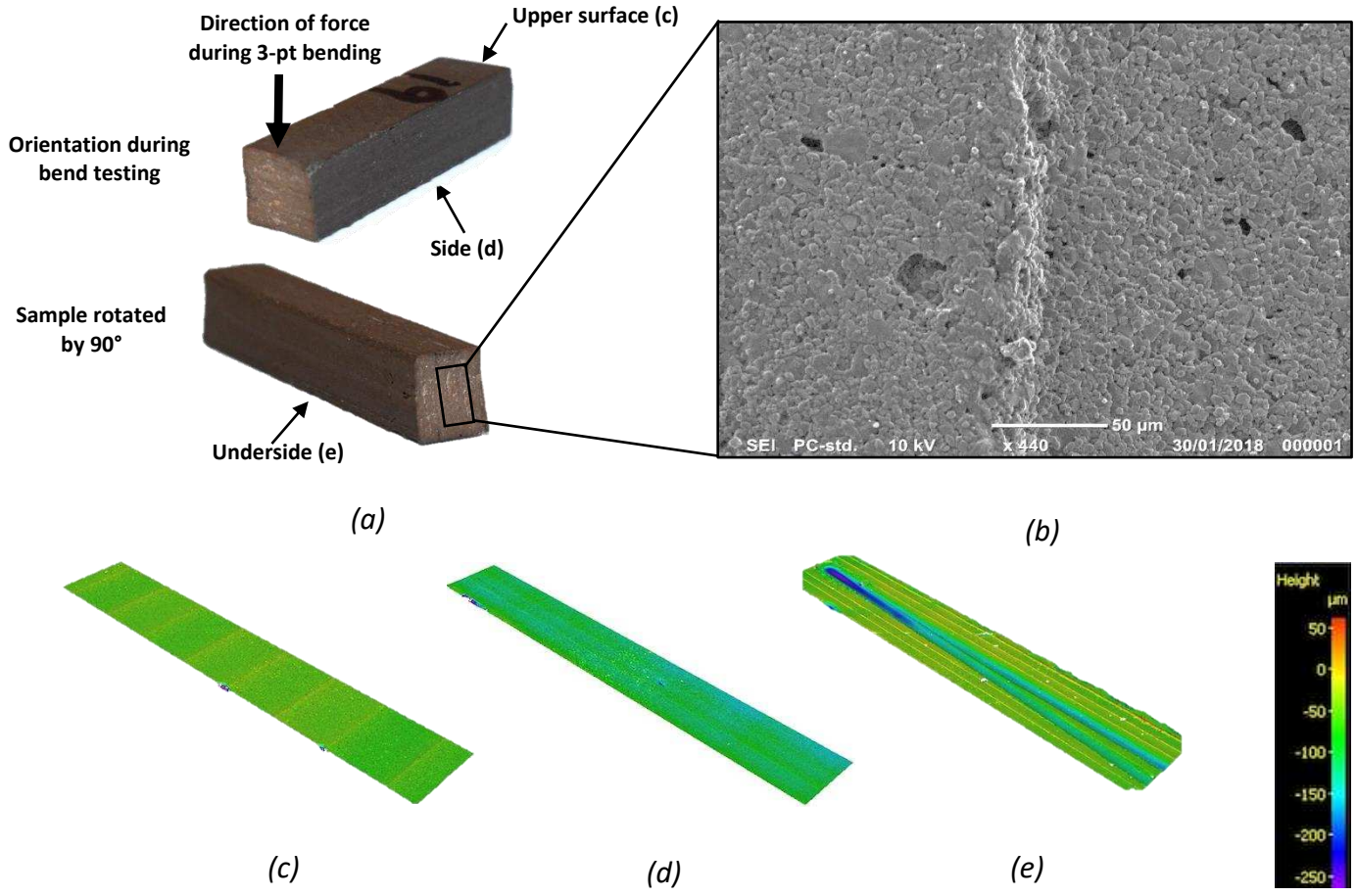

Figure 6 – (a) shows half of a bend test sample specimen and the sides that were analysed. The bend forced was applied perpendicular to the layers. (b) SEM imaging of the break interface on a bend test sample. A small amount of porosity is visible. The imaage confirms the creation of a monolithic component. (c) Shows the upper surface of the bend test sample. This component has been processed using end milling. (d) Shows

the side of the bend tast sample that has been side milled using climb milling. (e) shows the underside of the bend test sample that has been created on a PLA substrate created using material extrusion

Conclusion

This paper has presented the development of a new digitally driven, hybrid manufacturing system which has been validated by the production of high density ceramic components. The synergistic application of additive and subtractive manufacturing processes facilitates personalised production of components with an accuracy of $\pm 30\mu m$ with porosity <0.5%. The merits of post process machining have demonstrated improved tolerances and cosmetic appearance of components when compared with extrusion Additive Manufacturing. The optimised system yields components similar to conventional ceramic manufacturing technique yielding surface roughnesses as low as 1.01μm with mechanical bend strength of 253MPa. Analysis under SEM confirms the production of a monolithic ceramic components with no defects or voids visible in the interlayer region. It is envisioned this process will open up future applications in the production of engine and propulsion components, dental restorations and in electronics for the generation of insulators, conductors, capacitors, electromagnetic films and piezoelectric devices.

Acknowledgements

The author like to acknowledge the contributions of Chris Hampson, Marianne Sanderson, and Heather O'Brian of Morgan Advanced Materials.

References

Abel, J. et al. (2019) 'Fused Filament Fabrication (FFF) of Metal-Ceramic Components', Journal of Visualized Experiments. MyJoVE Corp, (143). doi: doi:10.3791/57693.

Bellini, A. (2002) Fused deposition of ceramics: a comprehensive experimental, analytical and computational study of material behavior, fabrication process and equipment design.

Brosha, E. L. et al. (2002) 'Development of ceramic mixed potential sensors for automotive applications', Solid State Ionics. Elsevier, 148(1–2), pp. 61–69.

Buchanan, R. C. (1986) Ceramic materials for electronics: processing, properties, and applications. Marcel Dekker, Inc.

Cesarano III, J. (1999) Robocasting of ceramics and composites using fine particle suspensions. Sandia National Labs., Albuquerque, NM (US); Sandia National Labs., Livermore, CA (US).

Correia, T. M. et al. (2013) 'A lead-free and high-energy density ceramic for energy storage applications', Journal of the American Ceramic Society. Wiley Online Library, 96(9), pp. 2699–2702.

Cox, S. C. et al. (2015) '3D printing of porous hydroxyapatite scaffolds intended for use in bone tissue engineering applications', Materials Science and Engineering: C, 47, pp. 237–247. doi: https://doi.org/10.1016/j.msec.2014.11.024.

Ćurković, L. et al. (2010) 'Flexural strength of alumina ceramics: Weibull analysis', Transactions of FAMENA. Facult of Mechanical Engineering and Naval Architecture, University of Zagreb, 34(1), pp. 13–18.

Deckers, J., Vleugels, J. and Kruth, J.-P. (2014) 'Additive manufacturing of ceramics: a review', Journal of Ceramic Science and Technology. Goeller Verlag GmbH, 5(4), pp. 245–260.

Denham, H. B. et al. (1998) 'Mechanical behavior of robocast alumina', in Solid Free. Fabr. Symp., Austin, TX, USA, pp. 589–596.

Edirisinghe, M. J. and Evans, J. R. G. (1986) 'Review: Fabrication of engineering ceramics by injection moulding. I. Materials selection', International Journal of High Technology Ceramics, 2(1), pp. 1–31. doi: https://doi.org/10.1016/0267-3762(86)90002-0.

Feilden, E. et al. (2016) 'Robocasting of structural ceramic parts with hydrogel inks', Journal of the European Ceramic Society, 36(10), pp. 2525–2533. doi: https://doi.org/10.1016/j.jeurceramsoc.2016.03.001.

Gao, W. et al. (2015) 'The status, challenges, and future of additive manufacturing in engineering', Computer-Aided Design, 69, pp. 65–89. doi: https://doi.org/10.1016/j.cad.2015.04.001.

Gibson, I., Rosen, D. W. and Stucker, B. (2010) Additive manufacturing technologies: Rapid prototyping to direct digital manufacturing. Springer US, Boston, MA.

Gonzalez, J. A. et al. (2016) 'Characterization of ceramic components fabricated using binder jetting additive manufacturing technology', Ceramics International, 42(9), pp. 10559–10564. doi: https://doi.org/10.1016/j.ceramint.2016.03.079.

Halloran, J. W. (2016) ‘Ceramic stereolithography: additive manufacturing for ceramics by photopolymerization’, Annual Review of Materials Research. Annual Reviews, 46, pp. 19–40.
Hammel, E. C., Ighodaro, O. L.-R. and Okoli, O. I. (2014) ‘Processing and properties of advanced porous ceramics: An application based review’, Ceramics International, 40(10, Part A), pp. 15351–15370. doi: https://doi.org/10.1016/j.ceramint.2014.06.095.
Hollister, S. J. (2005) ‘Porous scaffold design for tissue engineering’, Nature Materials. Nature Publishing Group, 4, p. 518. Available at: http://dx.doi.org/10.1038/nmat1421.
Klocke, F. and Ader, C. (2003) ‘Direct laser sintering of ceramics’, in Solid freeform fabrication symposium, pp. 447–455.
Klosterman, D. et al. (1998) ‘Interfacial characteristics of composites fabricated by laminated object manufacturing’, Composites Part A: Applied Science and Manufacturing, 29(9), pp. 1165–1174. doi: https://doi.org/10.1016/S1359-835X(98)00088-8.
Lorenz, K. A. et al. (2015) ‘A review of hybrid manufacturing’, in Solid Freeform Fabrication Conference Proceedings, pp. 96–108.
Martin, S. and Johannes, H. (2014) ‘Additive Manufacturing of Dense Alumina Ceramics’, International Journal of Applied Ceramic Technology. Wiley/Blackwell (10.1111), 12(1), pp. 1–7. doi: 10.1111/ijac.12319.
Naslain, R. et al. (2004) ‘Boron-bearing species in ceramic matrix composites for long-term aerospace applications’, Journal of Solid State Chemistry. Elsevier, 177(2), pp. 449–456.
Owen, D. et al. (2018) ‘3D printing of ceramic components using a customized 3D ceramic printer’, Progress in Additive Manufacturing. Springer, pp. 1–7.
Parra-Cabrera, C. et al. (2017) 3D printing in chemical engineering and catalytic technology: Structured catalysts, mixers and reactors, Chemical Society Reviews. doi: 10.1039/C7CS00631D.
Peng, E., Zhang, D. and Ding, J. (2018) ‘Ceramic Robocasting: Recent Achievements, Potential, and Future Developments’, Advanced Materials. John Wiley & Sons, Ltd, 30(47), p. 1802404. doi: 10.1002/adma.201802404.
Qian, B. and Shen, Z. (2013) ‘Laser sintering of ceramics’, Journal of Asian Ceramic Societies, 1(4), pp. 315–321. doi: https://doi.org/10.1016/j.jascer.2013.08.004.
Ribeiro, M. J., Ferreira, J. M. and Labrincha, J. A. (2005) ‘Plastic behaviour of different ceramic pastes processed by extrusion’, Ceramics International. Elsevier, 31(4), pp. 515–519.
Shui, A., Zeng, L. and Uematsu, K. (2006) ‘Relationship between sintering shrinkage anisotropy and particle orientation for alumina powder compacts’, Scripta Materialia, 55(9), pp. 831–834. doi: https://doi.org/10.1016/j.scriptamat.2006.07.026.
Sikalidis, C. (2011) Advances in Ceramics: Synthesis and Characterization, Processing and Specific Applications. IntechOpen. Available at: https://books.google.co.uk/books?id=HmmQDwAAQBAJ.
Soares, R. et al. (2018) ‘Large-area Ceramic Tooling Production through Hybrid Manufacturing’, in Direct Digital Manufacturing Conference. Berlin: Fraunhofer, pp. 3–8.
Tay, B. Y., Evans, J. R. G. and Edirisinghe, M. J. (2003) ‘Solid freeform fabrication of ceramics’, International Materials Reviews. Taylor & Francis, 48(6), pp. 341–370. doi: 10.1179/095066003225010263.
Wachtman, J. B., Cannon, W. R. and Matthewson, M. J. (2009) Mechanical properties of ceramics. John Wiley & Sons.
Wilkes, J. et al. (2013) ‘Additive manufacturing of ZrO2-Al2O3 ceramic components by selective laser melting’, Rapid Prototyping Journal. Emerald, 19(1), pp. 51–57. doi: 10.1108/13552541311292736.